size of the difference in power regardless of increase or decrease, were summed across all frequencies, from 0 to 48 kHz. The summed values were then integrated across all the analysis epochs of 500 msec and represented as the 1st SDVM. This index is thought to represent not only minor changes at the macro temporal level corresponding to musical notes, but also more complex changes at the micro temporal level that cannot be described by musical notes, such as reverberation and attack.

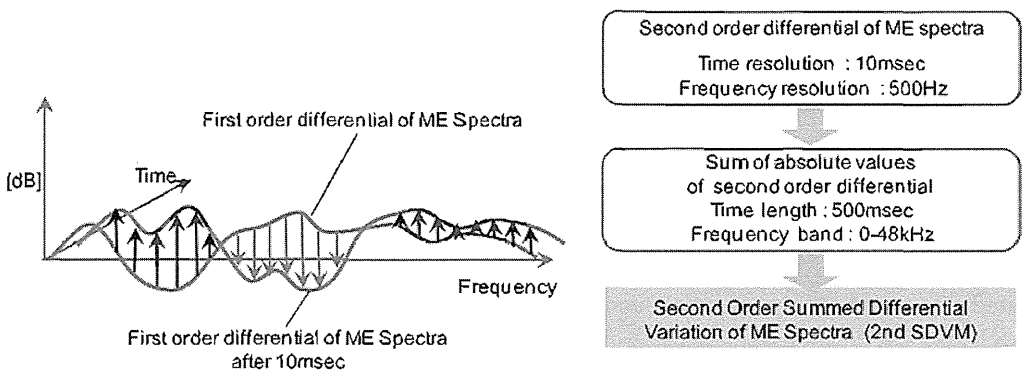

Fig. 2 The Second Order Summed Differential Variation of ME Spectra (2nd SDVM)

Although the 1st SDVM reflects the size of changes in power spectra, it does not reflect the complexity of such changes. In other words, the 1st SDVM shows a greater value for a monotonic increase, monotonic decrease or instantaneous major change corresponding to a musical note. To evaluate the complexity of changes in power spectra at the micro-temporal level, namely, the complexity in ups and downs of the power spectral array, we developed a second index, The Second Order Summed Differential Variation of ME Spectra (2nd SDVM) (Fig. 2). Similar to the 1st SDVM, these second order differentials were calculated and their absolute values were summed across the whole frequency range of 0 to 48 kHz and at the time epochs of 500 msec.

3. Results

Figure 3 shows ME spectral arrays of solo singing of traditional Georgian polyphony and that of solo singing of traditional Western opera. The traditional Georgian singing voice contains a rich, inaudible high-frequency component even beyond 40 kHz. In addition, even while a single keynote continues, the inaudible high-frequency component remains non-stationary and changes in complex ways. By contrast, the operatic *bel canto* singing voice does not contain any inaudible high-frequency components and is characterized by a periodical change of power spectra in an audible range, originating from a vibrato.

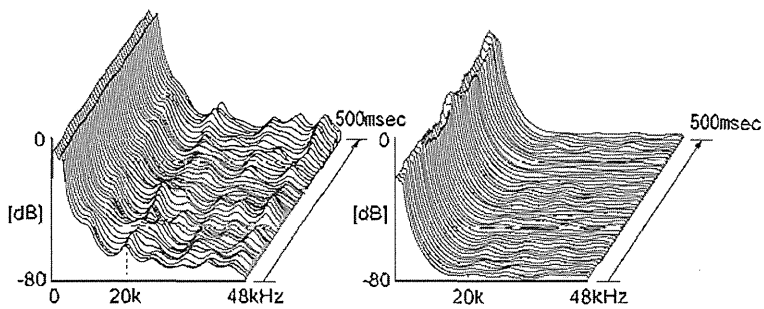

Fig. 3 ME spectral array of traditional Georgian singing voice and *bel canto* singing voice (solo)

Figure 4 shows 1st SDVM and the 2nd SDVM of Georgian and *bel canto* singing. Both indexes show greater values in Georgian singing than in *bel canto*. Such evidence supports the notion that traditional Georgian singing offers a more complex power spectral change.

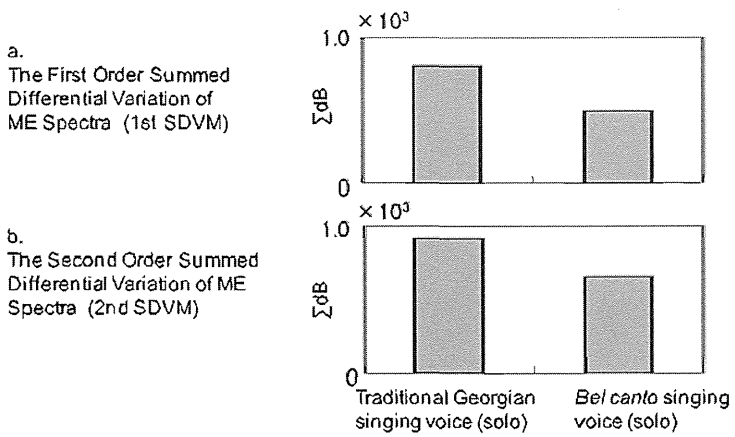

Fig. 4 Summed Differential Variation of ME Spectra
of traditional Georgian singing voice and *bel canto* singing voice (solo)

Figure 5 compares ME spectral arrays of solo and trio singing of traditional Georgian polyphony. We selected *Khasanbegura* for the trio. This piece contains more inaudible high-frequency components than does the solo. Moreover, spectral changes appear more prominent in the trio performance. Figure 6, with greater 1st SDVM and 2nd SDVM in the trio than in the solo corroborates such an interpretation. This finding suggests that the combination of three voices of traditional Georgian polyphony produces a more complex fluctuation in sound structure than does a solo performance.

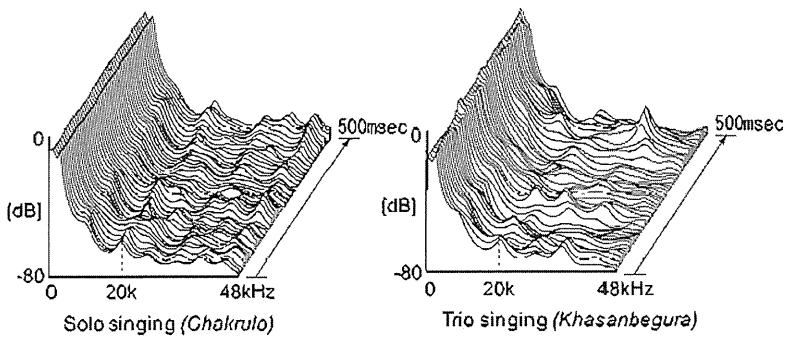

Fig. 5 ME spectral array of solo and trio singing in traditional Georgian polyphony

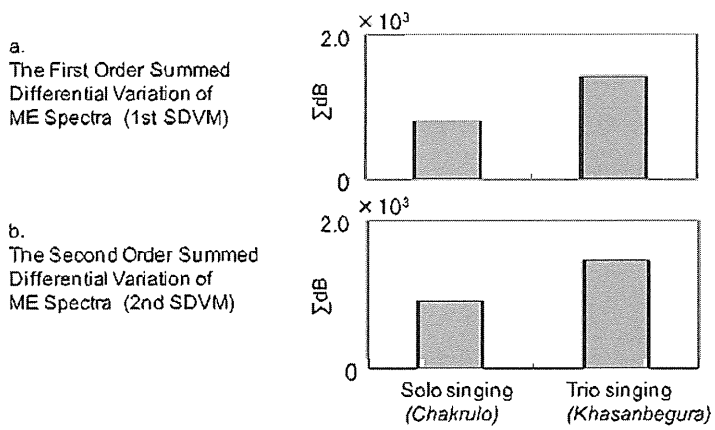

Fig. 6 Summed Differential Variation of ME Spectra
of solo and trio singing in traditional Georgian polyphony

4. Discussion

In this study, we have developed indexes for the quantitative evaluation of fluctuation of sound structure utilizing our previously developed ME spectral array method. The 1st SDVM Index includes both rough changes at the macro temporal level corresponding to musical notes and more subtle changes at the micro temporal level, such as reverberation and attack. At the same time, the 2nd SDVM more directly reflects the complexity of fluctuation of the ME spectral array at the micro-temporal level.

Using these two indexes, we compared traditional Georgian singing and *bel canto* singing both in solo performances. We found that both the 1st and 2nd SDVM showed greater values for traditional Georgian singing than for *bel canto*. In addition, such complexity was enhanced in trio performances in which three different voices sang together. The epochs analyzed in the present study correspond to a single musical note and thus did not contain any

changes in musical interval. Since *bel canto* singing contains vibrato, the rough change of the ME spectral array in the audible range below 20 kHz, upon visual inspection, seems more pronounced than in the Georgian singing. Nevertheless, both the 1st and the 2nd SDVM show greater values in traditional Georgian singing than in *bel canto*. This suggests that traditional Georgian singing contains an extremely rich fluctuation structure at the micro-temporal level, which surpasses the simple, periodic change of power spectrum in *bel canto*.

These characteristics of the sound structure of traditional Georgian singing correspond well to the biological concept of music proposed by Oohashi, which postulates that the essential characteristic of music is a non-stationary, continuously changing informational structure at the micro-temporal level. The Western European concept of music regards music as characterized by articulated musical tones with a stationary sound signal structure as a basic component; music and musical score can be mutually transposed. By way of contrast, as Georgians say, a Georgian folk singer never sings any phrase exactly the same way twice [5]. It is interesting that non-Western styles of singing, including the Georgian, emphasize the importance of improvisation by the singer rather than the musical score of the composer. The improvisation component may thus contribute to the unconsciously perceived, extremely complex fluctuations of the sound structure at the micro-temporal level .

Recent auditory physiology has revealed that the stationary character of sounds, such as stationary pitch and strength, is processed at an earlier stage in the auditory nervous system, whereas the non-stationary, complex character of sounds, such as fluctuation in amplitude and frequency, is processed throughout the whole auditory system including the higher brain system, which includes the thalamus and cerebral cortex [6]. Notably, the expressional strategy of traditional Georgian polyphony seems quite musically appropriate because it provides the listener with extremely rich non-stationary fluctuation that strongly activates the whole auditory nervous system.

5. Conclusion

We have developed two Summed DifferentialVariation of ME Spectra indices, which makes it possible to quantitatively evaluate the complexity of the fluctuation of the sound spectrum. Using these indices, we quantitatively compared the complexity of fluctuation of the power spectra at the micro-temporal level of traditional Georgian polyphony with that of the *bel canto* vocal performance. The power spectra of traditional Georgian polyphony are shown to offer more complex fluctuation than does a *bel canto* performance. This finding endorses the singular

importance of complex fluctuation as an expressional strategy of traditional Georgian polyphony.

6. References

[1] Oohashi, T., "*Oto to Bunmei* (Sound and Civilization)", Iwanami Shoten, 2003.

[2] Nishina, E. et al., "Hyper-symbolic sound structure of *Kartuli* Polyphonia", Proceedings of the Second International Symposium of Traditional Polyphony, 2004.

[3] Morimoto, M. et al., "Transcultural study on frequency and fluctuation structure of singing voices", Proceedings of the 18th International Congress on Acoustics (ICA2004), 55-58, 2004.

[4] Cura, J., DVD-audio *"Dramatic Hero-Verismo Opera Arias"*, Warner Music Japan, WPAS-10010, 2001.

[5] The International Centre for Georgian Folk Song, Preface to CDs *"Teach Yourself Georgian Folk Songs - Megrelian song"* (Collection of sheet music and Four Compact Discs), Publishing House Sakartvelos Matsne, 2005.

[6] Moore, B. C. J., "Hearing", Academic Press, 1995.

Development of a Brain PET System, PET-Hat: A Wearable PET System for Brain Research

Seiichi Yamamoto, *Member, IEEE*, Manabu Honda, Tutomu Oohashi, Keiji Shimizu, and Michio Senda

Abstract—**Brain functional studies using PET have advantages over fMRI in some areas such as auditory research in part because PET systems produce no acoustic noise during acquisition. However commercially available PET systems are designed for whole body studies and are not optimized for brain functional studies. We developed a low cost, small, wearable brain PET system named PET-Hat dedicated for brain imaging. It employs double counter-balanced systems for mechanical supports of the detector ring while allowing the subject some freedom of motion. The motion enables subject to be measured in the sitting position and move relatively freely with the PET during acquisition. The detector consists of a Gd_2SiO_5 (GSO) block, a tapered light guide and a flat panel photomultiplier tube (FP-PMT). Two types of GSO are used for depth-of-interaction (DOI) separation allowing the use of a small ring diameter without resolution degradation. The tapered light guide allows the use of larger GSO blocks with fewer FP-PMTs. Sixteen detector blocks are arranged in a 280 mm diameter ring. Transaxial and axial field-of-view (FOV) are 20 cm and 4.8 cm, respectively. Energy resolution of the block detectors was $\sim$ 15% full width at half maximum (FWHM) and timing resolution was $\sim$ 4.6 ns FWHM. Transaxial resolution and axial resolution at the center of the FOV were $\sim$ 4.0 mm FWHM and $\sim$ 3.5 mm FWHM, respectively. Sensitivity was 0.7% at the center of the axial FOV. Scatter fraction was $\sim$ 0.6. Hoffman brain phantom images were successfully obtained. We conclude that the PET-Hat is a promising, low cost, small, wearable brain PET system for brain functional studies.**

Index Terms—Brain, GSO, PET, PSPMT, wearable.

I. Introduction

In the early stage of human activation studies, positron emission tomography (PET) was used and many interesting brain functional insights were obtained [1]–[4]. After the introduction of the functional magnetic resonance imaging (fMRI) [5]–[6], most of these brain functional studies were shifted from PET to fMRI because the latter does not require positron radionuclides and thus does not require injections and has no radiation exposure. Furthermore, the activation sensitivity to the stimulation is generally higher than PET.

One drawback of the fMRI studies is the acoustic noise from the gradient sequence which makes it difficult to use for auditory experiments in human studies. Acoustic noise in MRI is usually more than 100 dB sound presser level (SPL) requiring headphones or bone conduction speakers for the auditory stimulation for fMRI studies, making it quite different from natural auditory conditions

Another drawback of the fMRI studies is that subject needs to lie in narrow and deep tunnel of the MRI making most of subjects uneasy, especially for subjects of claustrophobic show difficulty in measuring in MRI [7] and [8].

Brain functional studies using PET have advantages over fMRI in some areas such as auditory research of the brain because recent PET systems basically produce no acoustic noise with acquisition. However commercially available PET systems are designed for whole body studies and are not optimized for brain functional studies. Most of the commercial available PET systems are for imaging human body thus the diameter of the detector ring is large enough to image the human whole body increasing the cost and reducing the sensitivity of the PET system [9]–[12]. In addition, these commercially available PET systems measure subject lying on the bed in the tunnel of the PET. In the case of PET/CT system, the length of the tunnel became longer [9], [11] and the similar drawback to MRI system may be serious for claustrophobic subjects.

In the brain functional studies using delicate auditory stimulation, fMRI may not be a candidate for the imaging modality because of the serious acoustic noises and narrow spaces in the MRI measurements. PET will have an advantage for these applications. Commercially available whole-body PET systems are better, but like the MRI, subjects are measured while lying on the bed in the relatively long tunnel. In addition, the acoustic noise level in the tunnels of PET systems is much smaller than in MRI but relatively high from such as the cooling fans of the electronics in the gantry of the system.

For the measurements of sensitive stimulation such as the detection of hypersonic effect [13], subject must be measured in a silent and relaxed condition where the only target stimulus activates the subject. For the relax condition, it will be better to be measured in the sitting position. And if the detector ring can move with the subject's head, the subject may feel more relaxed during PET measurement while minimizing the head movement.

Some PET systems dedicated for brain measurements have been developed [14]–[18]. However in most of the PET system, subject must be lying on the bed during measurement while one

Manuscript received May 03, 2010; revised August 26, 2010; accepted January 03, 2011. This work was supported by the Japan Science and Technology Association through Core Research for Evolutional Science and Technology (CREST).

S. Yamamoto is with the Kobe City College of Technology, Nishi-ku, Kobe 651-2194, Japan (e-mail: s-yama@kobe-kosen.ac.jp).

M. Honda is with the National Center of Neurology and Psychiatry, Tokyo 187-8502, Japan (e-mail: honda@ncnp.go.jp).

T. Oohashi is with the Foundation for Advancement of International Science, Ibaraki 305-0062, Japan (e-mail: oohashi@fais.or.jp).

K. Shimizu and M. Senda are with the Institute of Biological Research and Innovation, Kobe, Hyogo 650-0047, Japan (e-mail: Shimizu@ibri.org; senda@ibri.org).

Color versions of one or more of the figures in this paper are available online at http://ieeexplore.ieee.org.

Digital Object Identifier 10.1109/TNS.2011.2105502

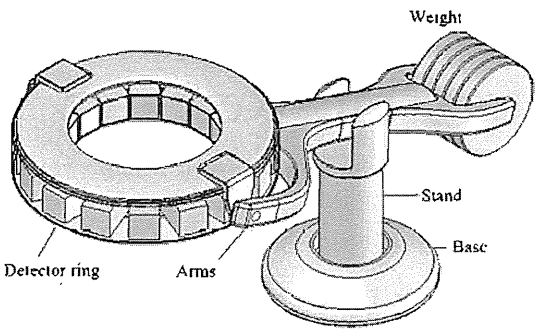

Fig. 1. Conceptual drawing of the PET-Hat.

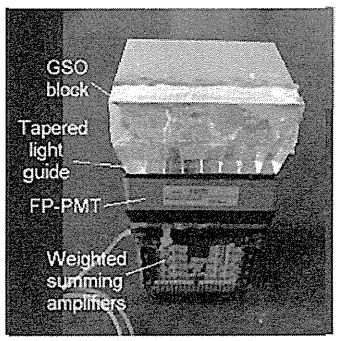

Fig. 2. Photograph of GSO block detector (from the top, GSO block, tapered light guide and FP-PMT) used for the PET-Hat. In photograph, printed boards of weighted summing amplifiers are shown under FP-PMT.

of the PET systems can measure in the sitting or standing position [18] but subject cannot move freely during measurement with the PET system. If the subject can move relatively freely while measurement, new neurological data that are impossible to measure such as measurements of blood flow changes during body or heads movement may become possible. Trying to satisfy these demands on the PET brain studies, we have developed a low cost, small and wearable PET system named PET-Hat.

II. Materials and Methods

A. Conceptual Design of the PET-Hat

Fig. 1 shows the conceptual drawing of the PET-Hat. The PET-Hat employs double counter-balanced systems in the mechanical supports. The detector ring of the PET system is supported by arms around which the detector ring can freely rotate during acquisition because the detector ring is balanced in the arms. The arms are supported by a stand and the detector weight is counterbalanced, which allows flee up and down motion. In addition, the stand can freely rotate around the base of the stand. These three motions enable subject to move relatively freely with the PET detector ring during acquisition by softly connecting the detector ring with the subject head.

B. GSO DOI Detector Block of the PET-Hat

The block detector for the PET-Hat consists of a Gd_2SiO_5 (GSO) block, a tapered light guide and a flat panel photomultiplier tube (FP-PMT). GSO was selected for the scintillators because the decay times can be controlled by the Ce concentration. Two types of GSO are stacked in the depth direction to form the depth-of-interaction (DOI) detector [19] and [20]. The DOI detection makes it possible to minimize the ring diameter of the PET system because it can reduce the spatial resolution degradation at off-center of the field of view (FOV). The tapered light guide is used to increase the size of the GSO blocks and reduce the number of FP-PMTs used for the PET-Hat.

The sizes of the GSO scintillators are 4.9 mm × 5.9 mm × 7 mm for inner layer (GSO with 1.5 mol% Ce: decay time of 40 ns) and 4.9 mm × 5.9 mm × 8 mm for outer layer (GSO with 0.4 mol% Ce: decay time of 80 ns), respectively. The inner layer means the layer closer to subject and the outer closer to the PSPMTs Light output difference between these two types of GSO were within 5%.

Depth length of these GSO scintillators was reduced to minimize the weight of the block detector for increasing the safety and decreasing the inertia of the PET-Hat. These GSO scintillators are combined into 11 × 8 matrix to form a block with size 55 mm (transaxial) × 48 mm (axial) . The GSO block is optically coupled to a FP-PMT through the tapered light guide. For the FP-PMTs, Hamamatsu H8500, 2-inches 8 × 8 multi-anode type [21] were used. The tapered light guide has 48 mm×48 mm area in the bottom (near to the FP-PMT) surface and 55 mm ×48 mm in the top (near to the GSO block) surface and 8 × 8 tapered cells are combined with multi-layer optical film (ESR: 3M) between them. Fig. 2 shows the assembled GSO block detector with GSO block, tapered light guide and FP-PMT.

C. Configuration of PET-Hat

Sixteen GSO DOI block detector was arranged in a ring with diameter 280 mm. The signals from each GSO block detector is weighted summed and is fed to 100 MHz analog to digital (A-D) converters of the data acquisition system [22] and signals are integrated with two different integration time (120 ns and 320 ns) [23], calculating the position using the Anger principle by field programmable gate array (FPGA). Also coincidences are measured digitally among eight groups (2 block detectors for 1 group) and stored in list mode to the personal computer (PC). The data acquisition system is basically the same as that used for small animal PET systems [22]. Time window was set to 16 ns and lower energy window to 350 keV. The gain of the FP-PMTs was manually tuned to be similar level before acquiring the position map of the block detectors for setting the position boundaries and energy windows. Data for normalization was measured using a 24 cm diameter ring source phantom containing F-18 solution.

Fig. 3 shows the developed PET-Hat system. It consists of a detector ring with double counter balanced arm, reclining chair and a notebook PC. End-shields made of two layers of 2 mm thick tungsten contained rubber were pasted at the lower edge of the detector ring. The end-shield covered scintillator blocks and the length was 2 cm.

The data acquisition system is encased under the detector ring. The control of the PET-Hat as well as data processing including image reconstruction is controlled by the notebook PC by wireless communication with a desk-top PC under the detector ring.

Fig. 4 shows photograph of the PET-Hat with a subject. Subject can sit on the reclining chair and the PET-Hat can be set

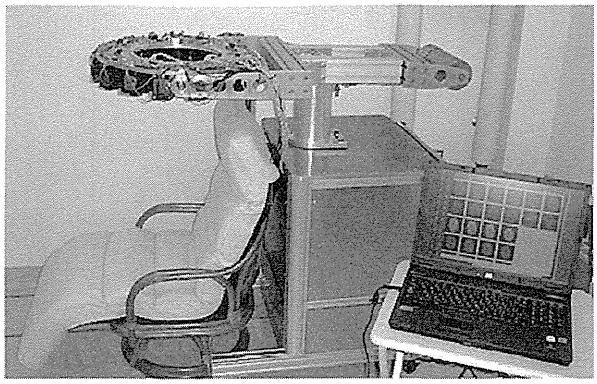

Fig. 3. Developed PET-Hat system.

Fig. 4. PET-Hat system with subject; front view (left) and side view (right).

from the top. By softly connecting the subject's head to detector ring using such as a straw hat that is attached at the detector ring of the PET-Hat, the subject can move relatively freely with the detector ring of the PET-Hat during acquisition.

Parts of a movie showing the movement of the PET-Hat with subject are shown in Fig. 5. The horizontal movement of the head and detector ring of the PET-Hat is shown in Fig. 5(a), the vertical movement in Fig. 5(b). The subject and the detector ring were connected with a straw hat that was connected with the detector ring of the PET-Hat.

D. Performance Evaluation of PET-Hat

1) Spatial Resolution: Spatial resolution measurements were made using a 1 mm diameter spherical shape Na-22 point source (radioactivity: 300 kBq) positioned at the center, 0 cm, 4 cm, 6 cm and 8 cm from the center of the FOV. Random coincidences were subtracted using the delayed data. At each position, more than 100 k counts were accumulated. List mode data were sorted into sinograms, after single slice rebinning with maximum ring difference of 4 and 2D filtered back-projection with ramp equivalent real space filter was used for reconstruction. Images were made with and without DOI correction.

2) Axial Resolution: Axial resolution was measured using the same Na-22 point source (1 mm diameter spherical shape point source, with radioactivity of 300 kBq). Images of the point source were reconstructed using 2D filtered back-projection with ramp equivalent real space filter and coronal images were re-sliced and evaluated.

3) Sensitivity: Sensitivity was measured by moving a Na-22 point source (1 mm diameter spherical shape point source, with

(a) (b)

Fig. 5. Parts of a movie showing movement of the PET-Hat with subject; horizontal movement (a) and vertical movement (b).

radioactivity of 300 kBq) in the axial direction and true coincidence rates were measured as a function of axial position.

4) Scatter Fraction: Scatter fraction was measured using a National Electrical Manufacturers Association (NEMA) 20 diameter, 70 cm long phantom using F-18 solution (radioactivity: $\sim$ 10 MBq) contained in the tube. The phantom was positioned at the center of the FOV. Scatter fraction was evaluated inside the FOV (20 cm). Scatter fraction was evaluated based on the NEMA NU 2001 standard [24].

5) Count Rate Performance: Count rate performance was measured using a NEMA standard 20 cm diameter, 70 cm height phantom contained $\sim$ 74 MBq F-18 solution. Following the decay of F-18, prompt, delayed and prompt minus delayed count rate were measured.

Noise equivalent count rate was also evaluated using the following formula with $k = 2$ because we used delayed coincidence for random correction.

$$\mathrm{NECR} = \frac{(\mathrm{T} \times \mathrm{T})}{(\mathrm{T} + \mathrm{kR} + \mathrm{S})}$$

where

T	true count rate
R	random rate
k	Delayed coincidence fraction
S	scatter rate

6) Hoffman Brain Phantom Imaging: The Hoffman brain phantom [25] contained 20 MBq of F-18 solution was positioned at the center of the FOV of the PET-Hat and measurements were made for 2 hours and total counts of $\sim$ 50 Mc were acquired. Data were reconstructed by 2D filtered back-projection using the normalization data. Analytical correction and single value subtraction were used for attenuation correction and scatter correction, respectively.

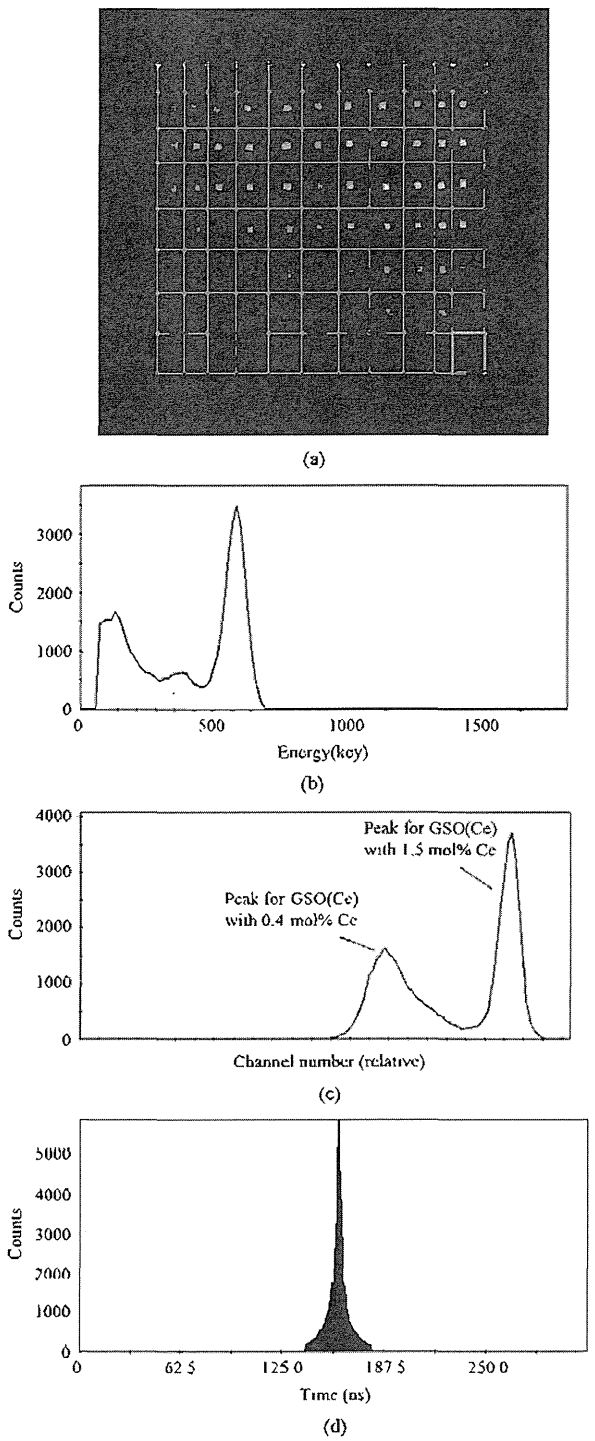

Fig. 6. Position map of the GSO block detector with position boundary (a) energy spectrum (b) pulse shape spectrum (c) and timing spectrum (d) of the GSO DOI block detector.

III. Results

A. Performance of the GSO DOI Block Detector

Fig. 6(a) shows the position map of the GSO block detector. Gamma photons form Cs-137 (661-keV) were irradiated from ~ 5 cm from the top of the GSO DOI block detector. The position map showed clear separation of all the GSO scintillators.

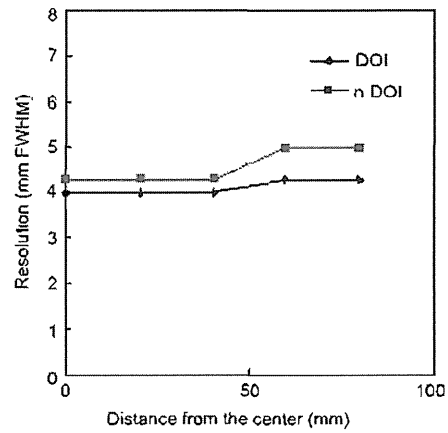

Fig. 7. Transaxial resolution as a function of distance from center.

The separation is good enough to divide each GSO scintillator using square boundaries. Fig. 6(b) shows an energy spectrum for one of the GSO scintillators in the block detector for Cs-137 gamma photons. The spectrum showed a single peak although the GSO scintillators consist of dual layer GSO with different decay times. Energy resolution was 15% full width at half maximum (FWHM).

Fig. 6(c) shows a pulse shape spectrum of one of the GSO scintillators of the block detector for Cs-137 gamma photons. The pulse shape spectrum showed good separation of these two types of GSO with different decay times. The right peak in Fig. 6(c) is the GSO with 1.5 mol % Ce and left is the with 0.4 mol% Ce. The peak to valley (P/V) ratio among these peaks was 14. With this P/V ratio, the percent error in separation of two layers is almost zero.Fig. 6(d) shows the timing spectrum measured using a positron source between GSO block detectors. Timing resolution was 4.6 ns FWHM. The timing spectrum showed wider distribution at the bottom area so time window was set relatively wider (16 ns).

B. Performance of PET-Hat System

1) Spatial Resolution: Fig. 7 shows transaxial resolution as a function of distance from the center. Transaxial resolutions at the center of the FOV were 4.0 mm FWHM with DOI correction and 4.3 mm FWHM without DOI correction at the center of the FOV and 4.2 mm FWHM with DOI correction and 5.0 mm FWHM without DOI correction at 8 cm from the center of the FOV.

2) Axial Resolution: The axial resolution at the center of the FOV was 3.5 mm FWHM.

3) Sensitivity: Sensitivity profile as a function of the axial position is shown in Fig. 8. Sensitivity for point source was 0.72% at the center of the axial FOV. The count rate outside the axial FOV (48 mm) is from the scatter coincidence between detector blocks when the source is outside FOV.

4) Scatter Fraction: Scatter fraction as a function of slice number is shown in Fig. 9. Average scatter fraction was 0.6.

5) Count Rate Performance: Count rate characteristic is shown in Fig. 10. The maximum prompt minus delayed count rate was ~ 12 kcps and NECR was 0.82 kcps within the measured activity range.

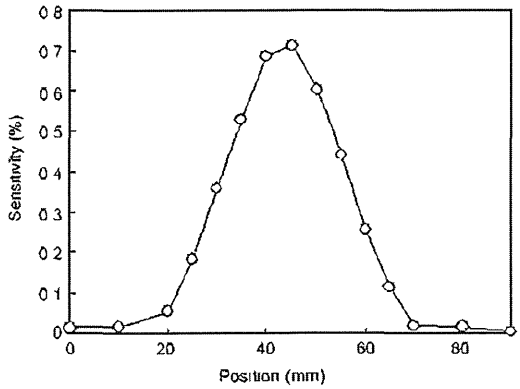

Fig. 8. Sensitivity profile as a function of the axial position.

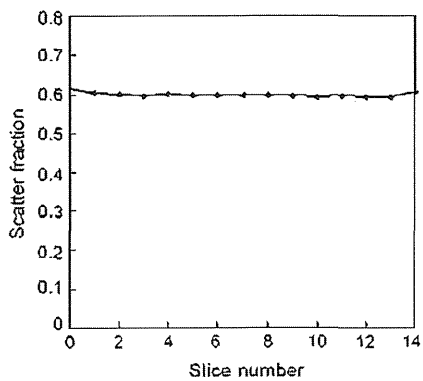

Fig. 9. Scatter fraction as a function of the slice number.

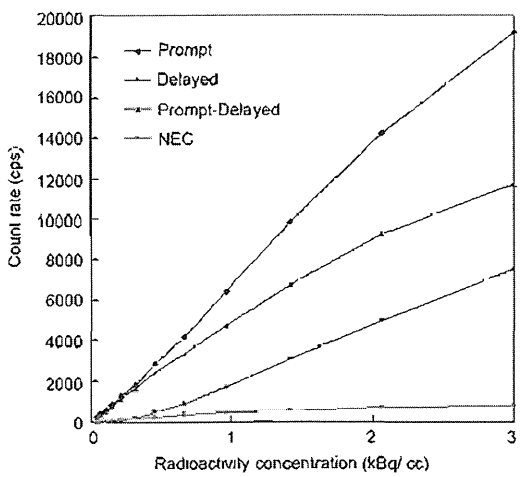

Fig. 10. Count rate characteristic measured using 20 cm diameter, 70 cm height cylindrical phantom.

6) Images of the Hoffman Brain Phantom: Images of the Hoffman brain phantom at the central 9 slices are shown in Fig. 11. In the images we can observe the small structures of the gray matter regions of the phantom.

IV. Discussion

We successfully developed a wearable brain PET system. The PET-Hat could move relatively freely with subject movement.

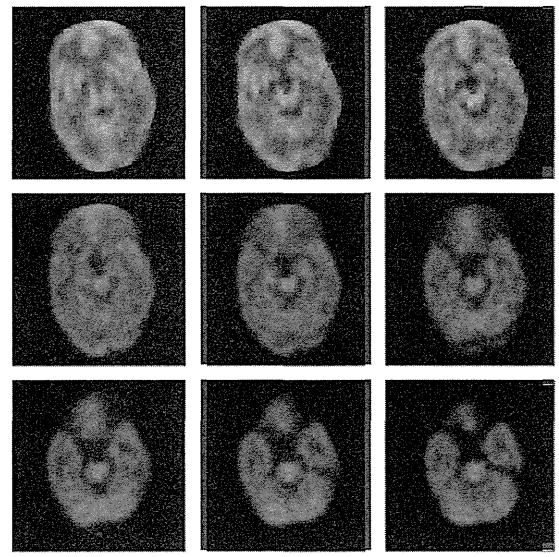

Fig. 11. Hoffman brain phantom images contained F-18.

However the rotation or sideways neck motion produced the sift of position in the straw hat (connecting part of PET-Hat and head) that may produce image degradation from subject movements. For more free movement, rotation of the detector ring with the subject can add one more free movement of the subject with some sacrificing of the increase of the weight of the detector ring. The increase of the weight increases the inertia thus increases force for starting and stopping the movement of the detector ring.

The sensitivity of the system can be increased by several ways; increase the depth of the scintillators, use of the dense, high atomic number scintillators such as LGSO, LYSO, or LSO and increase the axial FOV. These attempts to increase the sensitivity also increase the weight of the detector ring that will require more safety mechanism for the mechanical support such as counter balanced system.

In this PET-Hat system, the effect of DOI detection was not very obvious because the depth of the GSO scintillators were relatively short, 7 mm and 8 mm. If we select GSO scitnillators with longer depth, the difference of the spatial resolution with and without DOI detection would be more attractive. However in this case, the weight of the detector ring would more heavy.

The scatter fraction of the system was relatively high, higher than the whole body PET systems [9]–[12]. The reasons are the end-shield of the detector ring is set only the lower side of the detector ring and its thickness and length are small. For the brain studies, only the scatter from the lower side of the ring will be important because there is no activity on the upper side of the detector ring. Thus the scatter contribution of the human studies will be smaller than that used NEMA phantom. The use of an additional gamma shield from the body such as gamma absorb apron may be useful for the human studies.

The image quality of the Hoffman brain phantom shown in Fig. 11 was not very attractive. One reason is the low sensitivity of the system with the small axial FOV (44 mm) and the short scintillators depth (15 mm). The other reason is the low NECR of the system because of the high scatter fraction and random

rate. Using the filtered back-projection for the image reconstruction is another reason of the limited quality of the phantom images. Optimization of the system parameters such as lower energy level or time window may improve the image quality in somehow. Also applying an iterative image reconstruction will improve the image quality of the PET system.

V. Conclusion

We have successfully developed the PET-Hat for brain research. The PET-Hat could be measured in the sitting position of the subject and could move with the subject. We conclude that the PET-Hat is promising, low cost, small size, wearable brain PET system for brain functional studies.

Acknowledgment

The authors would like thank to Mr. Ohta of Eiko-Sangyo Co. for designing and constructing the mechanical part of the PET-Hat system.

References

[1] P. T. Fox, M. A. Mintun, M. E. Raichle, F. M. Miezin, J. M. Allman, and D. C. Van Essen, "Mapping human visual cortex with positron emission tomography," *Nature*, vol. 323, pp. 806–809, Oct. 1986.

[2] S. E. Petersen, P. T. Fox, A. Z. Snyder, and M. E. Raichle, "Activation of extrastriate and frontal cortical areas by visual words and word-like stimuli," *Science*, vol. 249, no. 4972, pp. 1041–1044, 1990.

[3] M. Corbetta, F. M. Miezin, S. Dobmeyer, G. L. Shulman, and S. E. Petersen, "Attentional modulation of neural processing of shape, color and velocity in humans," *Science*, vol. 248, no. 4962, pp. 1556–1559, 1990.

[4] P. T. Fox, M. E. Mintun, M. E. Raichle, and P. P. Herscovitch, "A noninvasive approach to quantitative functional brain mapping with H2 (15)O and positron emission tomography," *J. Cereb. Blood Flow Metab.*, vol. 4, no. 3, pp. 329–333, 1984.

[5] S. Ogawa, T. M. Lee, A. R. Kay, and D. W. Tank, "Brain magnetic resonance imaging with contrast dependent on blood oxygenation," *Proc. Natl. Academy Sciences USA*, vol. 87, no. 24, pp. 9868–9872, 1990.

[6] S. Ogawa, T. M. Lee, and G. Barrere, "The sensitivity of magnetic resonance image signals of a rat brain to changes in the cerebral venous blood oxygenation," *Magn. Reson. Med.*, vol. 29, no. 2, pp. 205–210, 1993.

[7] I. Eshed, C. E. Althoff, B. Hamm, and K. G. Hermann, "Claustrophobia and premature termination of magnetic resonance imaging examinations," *J. Magn. Reson. Imag.*, vol. 26, no. 2, pp. 401–404, 2007.

[8] S. Thorpe, P. M. Salkovskis, and A. A. Dittner, *Magn. Reson. Imag. Claustrophobia in MRI: The Role of Cognitions*, vol. 26, no. 8, pp. 1081–1088, 2008.

[9] M. Teräs, T. Tolvanen, J. J. Johansson, J. J. Williams, and J. Knuuti, "Performance of the new generation of whole-body PET/CT scanners: Discovery STE and discovery VCT," *Eur. J. Nucl. Med. Mol. Imag.*, vol. 34, no. 10, pp. 1683–1692, 2007.

[10] K. Matsumoto *et al.*, "Performance characteristics of a new 3-dimensional continuous-emission and spiral-transmission high-sensitivity and high-resolution PET camera evaluated with the NEMA NU 2-2001 standard," *J. Nucl. Med.*, vol. 47, no. 1, pp. 83–90, 2006.

[11] S. Surti, A. Kuhn, M. E. Werner, A. E. Perkins, J. Kolthammer, and J. S. Karp, "Performance of philips gemini TF PET/CT scanner with special consideration for its time-of-flight imaging capabilities," *J. Nucl. Med.*, vol. 48, no. 3, pp. 471–480, 2007.

[12] G. Brix *et al.*, "Performance evaluation of a whole-body PET scanner using the NEMA protocol. National electrical manufacturers association," *J. Nucl. Med.*, vol. 38, no. 10, pp. 1614–1623, 1997.

[13] T. Oohasi *et al.*, "In audible high-frequency sound affect brain activity: Hypersonic effect," *J. Neuriphysiol.*, vol. 83, no. 6, pp. 2548–2558, 2000.

[14] J. S. Karp, S. Surti, M. E. Daube-Witherspoon, R. Freifelder, C. A. Cardi, L. E. Adam, K. Bilger, and G. Muehllehner, "Performance of a brain PET camera based on anger-logic gadolinium oxyorthosilicate detectors," *J. Nucl. Med.*, vol. 44, no. 8, pp. 1340–1349, 2003.

[15] H. W. de Jong, F. H. van Velden, R. W. Kloet, F. L. Buijs, R. Boellaard, and A. A. Lammertsma, "Performance evaluation of the ECAT HRRT: An LSO-LYSO double layer high resolution, high sensitivity scanner," *Phys. Med. Biol.*, vol. 52, no. 5, pp. 1505–1526, 2007.

[16] E. Yoshida *et al.*, "Design and inital evaluation of a 4-layer DOI-PET system. The jPET-D4," *Igaku Butsuri.*, vol. 26, no. 3, pp. 131–140, 2006.

[17] D. L. Bailey, T. Jones, T. J. Spinks, M. C. Gilardi, and D. W. Townsend, "Noise equivalent count measurements in a neuro-PET scanner with retractable septa," *IEEE Trans. Med. Imag.*, vol. 10, no. 3, pp. 256–260, 1991.

[18] M. Watanabe *et al.*, "A new high-resolution PET scanner dedicated to brain research," *IEEE Trans. Nucl. Sci.*, vol. 49, no. 3, pp. 634–639, Jun. 2002.

[19] S. Yamamoto and H. Ishibashi, "A GSO depth of interaction detector for PET," *IEEE Trans. Nucl. Sci.*, vol. 45, no. 3, pp. 1078–1082, Jun. 1998.

[20] S. Yamamoto, "A dual layer DOI GSO block detector for a small animal PET," *Nucl. Instrum. Methods Phys. Res. A*, vol. A598, pp. 480–484, 2008.

[21] R. Pani, M. N. Cinti, R. Pellegrini, C. Trotta, G. Trotta, L. Montani, S. Ridolfi, F. Garibaldi, R. Scafè, N. Belcari, and A. D. Guerra, "Evaluation of flat panel PMT for gamma ray imaging," *Nucl. Instrum. Methods Phys. Res. A*, vol. A504, pp. 262–268, 2003.

[22] S. Yamamoto, H. Mashino, H. Kudo, K. Matsumoto, and M. Senda, "A dual layer GSO PET system for small animal: K-PET II," *IFMBE Proc.*, vol. 14, pp. 1712–1715, 2007.

[23] S. Yamamoto, "Optimization of the integration time of pulse shape analysis for dual layer detector with different amount of Ce," *Nucl. Instrum. Methods Phys. Res. A*, vol. A587, pp. 319–323, 2008.

[24] M. E. Daube-Witherspoon *et al.*, "PET performance measurements using the NEMA NU 2-2001 standard," *Nucl. Med.*, vol. 43, no. 10, pp. 1398–1409, 2002.

[25] E. J. Hoffman, P. D. Cutler, W. M. Digby, and C. J. Mazziotta, "3-D phantom to simulate cerebral blood flow and metabolic images for PET," *IEEE Trans. Nucl. Sci.*, vol. 37, no. 2, pp. 616–620, Apr., 1990.

ハイパーソニック・エフェクト応用による音響療法の展望

Perspective of "sound therapy" as an application of hypersonic effect.

○仁科エミ[1]、八木玲子[2]、河合徳枝[2]、森本雅子[3]、本田　学[3,4]、大橋　力[2]
[1]放送大学／総合研究大学院大学、[2]国際科学振興財団
[3]国立精神・神経医療研究センター神経研究所、[4]科学技術振興機構 CREST
NISHINA Emi[1], YAGI Reiko[2], KAWAI Norie[2], MORIMOTO Masako[3],
HONDA Manabu[3,4] & OOHASHI Tsutomu[2]
[1] The Open University of Japan / SOKENDAI, [2] Foundation for Advancement of International Science,
[3] National Center of Neurology and Psychiatry, [4] CREST, JST

知覚限界をこえる高周波を豊かに含む音は、環境適応、生体防御、美と快の感覚などを一括して制御する基幹脳ネットワークの血流を増大させることを私たちは見出した。このハイパーソニック・エフェクトについて、とくに脳機能に及ぼす影響に重点をおいて紹介するとともに、その応用について報告する。

Key Words: Hypersonic effect, Sound therapy, high frequency components, fundamental brain

1　はじめに

私たちの研究リーダー大橋は、作曲家山城祥二として音楽スタジオでレコード制作を手掛けるなかで、人間の可聴域上限をこえる高複雑性の超高周波成分を強調すると、音の味わいが玄妙に高まることを見出した[1]。そしてこの音楽家としての主観的一人称的体験に基づく内観的認識を、脳科学を中心とする実験科学によって、客観的実証的に解明することに取り組んだ。その結果、私たちは、知覚限界をこえる超高密度複雑性の音が基幹脳ネットワークを活性化させ、それによって生理・心理・行動に及ぶ多様でポジティブな効果（ハイパーソニック・エフェクト）が導かれることを見出した。

超高周波によって活性化される基幹脳ネットワークは、環境適応、生体防御、美と快の感覚などを一括して制御する中枢であり、体と心の健やかさを保つ上できわめて重要な働きをしている。そこで私たちは、このハイパーソニック・エフェクトを応用した音響療法を構想し、予備的な検討に着手している。

本稿では、この取り組みの基礎となる現象・ハイパーソニック・エフェクトを、とくに脳機能に及ぼす影響に重点をおいて紹介するとともに、その応用について報告する。

2　ハイパーソニック・エフェクトとは何か

2.1　ハイパーソニック・サウンドとは

よく知られているように人間の可聴域の上限は一般的に20kHzを超えない。一方、最先端の超広帯域音響収録分析システムをもちいて改めて調べてみると、人類の進化の揺籃となった熱帯雨林の環境音や、伝統に磨かれた民族音楽のなかには、複雑なゆらぎをもった人間には音として聴こえない超高周波成分を豊かに含むものが少なからず存在している[2]。その周波数帯域は20kHzを大幅に上まわり、時として100kHz以上に及ぶ。このような自然音を、私たちは＜ハイパーソニック・サウンド＞と名付けた。なお、ハイパーソニック・サウンドは、都市環境音やピアノなどの近代楽器音、ＣＤ、携帯プレーヤー、デジタル放送の音には含まれていないことに注意を要する（Fig.1）。

2.2　脳波を指標として現象の動的特性を捉える

このようなハイパーソニック・サウンドに囲まれているときの人間の状態を把握するために、私たちは、近年の著しい脳科学研究手法に注目した。脳の活動は、原理的に二つの側面からの非侵襲計測が可能になっている。第一は神経放電を捉えるもので、

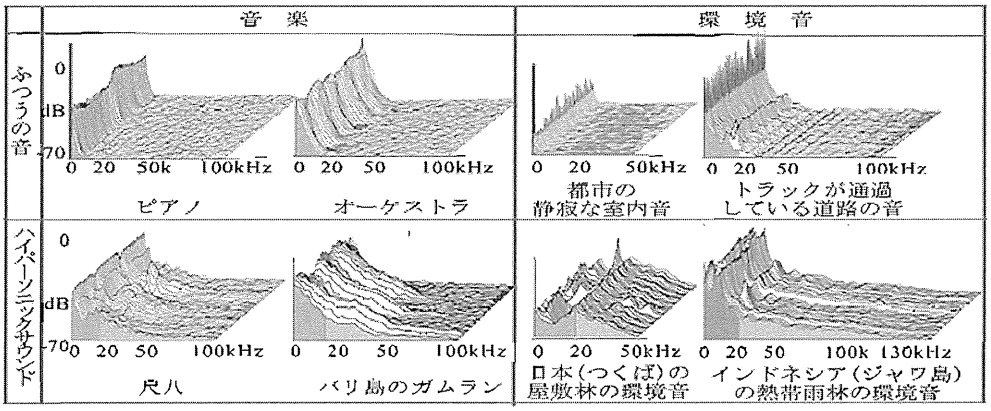

Fig.1 ハイパーソニック・サウンドとは

脳電位がその対象となり、頭皮表面に伝わる電位そのものを計測する脳波(EEG)、電気現象に伴って発生する磁気を計測する脳磁図(MEG)が実用水準にある。脳電位という指標は脳活性の時々刻々の遷移を直接に反映し、正確な時間情報を得るのに適している。第二は、神経活動の実体が生化学反応であるため、物質代謝を支える血流の変化としてこれを捉えるものである。ラジオアイソトープでトレースするポジトロン断層撮像法(PET)や、血液成分固有の分子の磁気的挙動に注目する機能的磁気共鳴画像法(fMRI)があり、いずれも活性化する脳領域について精密な空間情報を与えてくれる。私たちは、この両側面からアプローチした。

超高周波の共存によって音の趣きが増す、というレコード制作過程での大橋の体験を当時の先端的な脳科学の知見に照らし、それが脳の報酬系の活性化を反映して脳波α波を増強するであろう可能性を想定した。つまり、超高周波を含む音と含まない音とで、脳波α波の発現状態に差が認められるかどうかを検討することを構想した。この場合、報酬系の活性化を妨げるような計測環境下では、その負の影響に感性反応が埋没して結果が現れにくくなる恐れがある。ところがこの研究に着手した段階では、医療現場の脳波計測にはこうした感性反応に関わる配慮がほとんど認められず、緊張や恐怖などのネガティブな情動反応が報酬系の活性化を妨げる可能性が濃厚だった。そこで、こうした影響を排除し、快適な環境で音楽を楽しむことができる脳波計測実験環境を特別に構築した。さらに、従来の医療用脳波計測手法を抜本的に見直し、FM多重送信によってワイアレスでデータを送信するテレメトリー・システムの導入・改良により、ノイズ発生を避けるとともに被験者の行動を計測時の拘束から解放するなど、実験条件に細かい工夫を重ねた[3]。

この系を用い、高周波を豊富に含むインドネシア・バリ島のガムラン音楽（200 秒）を呈示音源として、バイチャンネル再生系[4]により、①26kHz 以上の超高周波成分と可聴音を主とする 26kHz 以下の成分とが共存するフルレンジ音（FRS)、②26kHz 以下のハイカット音（HCS)、③暗騒音（環境雑音）のみのベースラインの 3 条件を構成し、それぞれの条件下の脳波を連続して記録し、α 波帯域パワーについて頭皮上の脳電位図を描き統計検定を行った。被験者位置での呈示音のスペクトルを Fig.2 に示す。

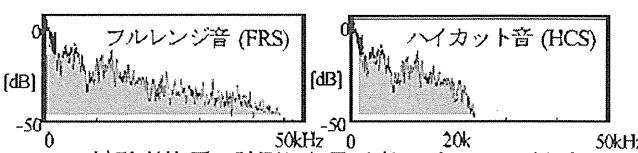

Fig.2 被験者位置で計測した呈示音のパワースペクトル (200 秒平均)

その結果、Fig.3 に示すように、α波のパワーはフルレンジ音呈示開始から 20〜30 秒間かけて顕著に増加し、その活性水準が保たれる。ハイカット音に切りかえると約 100 秒近くその活性が残留し一種の「脳活性の残像」を構成したのち減少する、という特異な経過が認められた。そこで、この残像が消え尽きる音呈示後半の時間領域についてα波パワーを数量化して比較したところ、フルレンジ音すなわちハイパーソニック・サウンドによってα波パワーが統計的有意に増強されるという事実を初めて見出すことができた[3]。

2.3 ポジトロン断層撮像法による検討

脳波が時間分解能にきわめて優れているのに対して、領域脳血流（rCBF）は、脳内活性化領域について高度に精緻な空間的情報を与えてくれる。私たちは、ハイパーソニック・エフェクトの発現に関与す

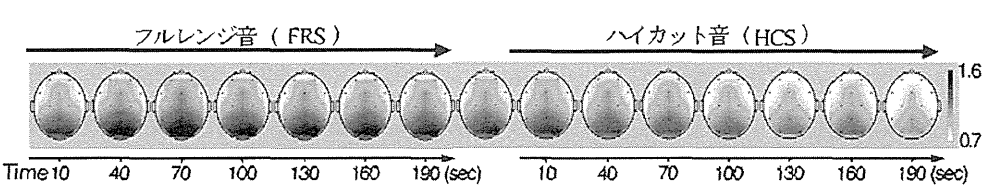

Fig.3 ハイパーソニック・サウンドは時差を伴って脳波α波を増大させる

る脳領域を、PETを用いた脳血流計測により検討した[5]。トレーサーには$H_2{}^{15}O$を用い、脳波の場合に準じてPET測定室の環境を細部にわたり改造・快適化し、音源にも同じガムラン音楽を採用して、一連の実験を3ヶ年にわたって行った。被験者は健常な日本人男女12名であり、京都大学医学部倫理委員会の承認に基づいて実験を実施した。呈示音は、実験室の暗騒音に加えてハイカット音、超高周波成分のみ、フルレンジ音を呈示、各条件間のrCBFを詳細に比較検討した。まず、SPMソフトウェア[6]をもちいて条件間の血流の差を統計的に検定し画像として描出した。その結果、フルレンジ音を呈示したときには、ハイカット音を呈示したときに比べて脳深部にある脳幹と視床の血流が統計的有意に増大するという注目すべき事実が見出された。しかも、それらの部位は、聴覚神経系の中継点となる下丘や内側膝状体とは一致しない。つまり、聴覚系に属する領域では、超高周波成分があるかないかによって神経活動に変化は認められない。この特異な脳深部の活性増大は、超高周波単独の呈示では観察されなかっただけでなく可聴音単独の呈示では、この部位の活性は逆に下降し、ベースライン条件に比較しても有意に抑制されることが判明した[6]。

SPMによる解析は、活性部位の頂上をいわばピンポイント的に厳密に描出する。それに対して頂上から裾野そして山脈のつながりを包括的に捉えるには、主成分分析法が適している。これによって、呈示される音の違いに対応して互いに関連し合いながらまとまって活動する神経回路の全体像を描出した[7]。その結果、最大の活性変化を示す第一主成分として、可聴音の存在に対応して、古典的聴覚系を構成する側頭葉の聴覚野皮質を含む領域が当然ながら抽出された。その次に大きな変化を示す第二主成分として、ハイパーソニック・サウンドの存在に対応して、脳幹、視床、視床下部、上部脳幹から発し前帯状回および前頭前野へと拡がるモノアミン系と推定される神経ネットワーク、さらに頭頂葉楔前部が抽出されるという注目すべき結果が得られた。脳幹、視床やそこから大脳辺縁系、大脳皮質へと投射するモノアミン系ネットワークは情動・感性にかかわる報酬系に属し、美しさ快さを司る。また、脳幹と視床下部は、生体制御系すなわち自律神経系、免疫系、内分泌系の最高中枢として健康を司る。第二主成分として抽出されたこれら二つの脳機能が一体化した系はまさに人の心と体の根幹を担うものであり、基幹脳ネットワークと呼ぶにふさわしい（Fig.4）。

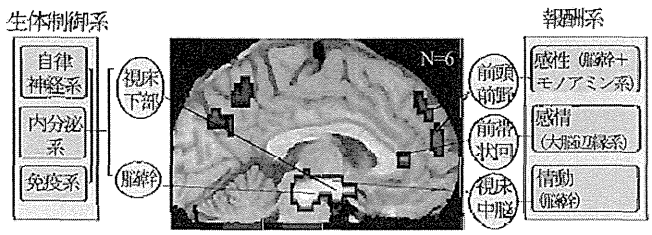

Fig. 4 ハイパーソニック・サウンドは基幹脳ネットワークの血流増加を導く

主成分分析と同時に行った脳波解析により、基幹脳ネットワーク全体の活性が、頭皮上特定の領域から抽出される特定周波数帯域の脳波α波のパワーと高度に有意に相関していることが明らかとなった。この知見により、頭皮表面上から比較的容易に計測できる脳波α波を指標として基幹脳活性を高い信頼性で推計することが可能になった。

さらに、基幹脳をネットワークの活性化を反映した領域脳血流値の増大、脳波α波の増強とともに、ハイパーソニック・サウンドによって、NK細胞など免疫活性の上昇、アドレナリンなどストレス性ホルモンの減少、音のより快く美しい受容の誘起、音をより大きく聴く接近行動の誘導など多岐にわたる反応が導かれることがわかった[7, 8]。しかも、ハイパーソニック・エフェクトを発現させるためには、可聴音を聴覚系に呈示するとともに、高周波を体表面に印加する必要があることも見出された[9]。

3　基幹脳活性化と音響療法

3.1　基幹脳活性不全と現代病

ハイパーソニック・サウンドによって活性化される基幹脳ネットワークは、環境適応や生体防御に当たり健康を司る「生命活動」と、美と快の感覚を発

生させ感性・感情を司る「精神活動」とを連携して制御する中枢として働いている。そのため、基幹脳の活性化は自律神経系・内分泌系・免疫系、そして報酬系の活動を包括的に向上させ、体には健康、心には知覚の鋭敏化に加えて美と快そして安らぎをもたらす。一方、この基幹脳の活性不全が、がん、高血圧、認知症、うつ、自殺、暴力など、社会を窮地に陥れている多くの現代病の引金になっていることが、最近、多方面から相次いで報告されている。

しかも、超高周波成分を除いた音を呈示した時、音楽を呈示していない時よりも基幹脳ネットワークの活性が顕著に抑制されたことは看過できない。この神経ネットワークの機能はさまざまな生命活動に密接に関与しており、その活性不全がいわゆる現代病の誘発可能性と関連して近年急速に注目されつつあることからも、それがもたらす直接間接の影響に十分な注意を払う必要がある。

3.2 ハイパーソニック・エフェクトの社会応用

以上から私たちは、ハイパーソニック・エフェクトによる基幹脳の活性化には、心身に及ぶ現代の深刻な病理に対する防御効果が期待されると考え、その社会応用に取り組んでいる。すでに、オーディオ・システムの音質改善や街の音環境の改善[10]、パッケージメディア[11]への応用は軌道に乗りつつある。

そして次の段階として私たちはいま、ハイパーソニック・エフェクトによる基幹脳活性化を、現代病の防御に本格的に応用する方途を検討している。これまで行われている音楽療法が、意識すなわち知覚でき意識される音楽の効果を応用するのに対して、私たちが構想するアプローチは、知覚できず意識されない超高周波の効果に注目したものである。そこで、これを音楽療法と区別するために、<音響療法>と呼ぶことにする。音響療法では、人類の遺伝子を育んだ熱帯雨林環境音をはじめ、人類史的に安全性が保証された自然音の高忠実度録音物を用いる。自然環境音に対する個人の嗜好の差は音楽よりも小さいので、音楽療法に比べると個人の嗜好の差の影響を受けにくい可能性がある。もしこのようなハイパーソニック応用が実現するならば、薬物を使わないため副作用がなく、薬物に劣らない作用を発揮するこれまで例のないアプローチが実現する可能性がある。

4 おわりに

ハイパーソニック・エフェクトを応用した音響療法という構想は、現代病の起源を「人間と情報環境との不適合による基幹脳の活性低下」という根本原因に遡って捉え、先端的情報技術を駆使した基幹脳活性の回復によってその解消をめざすものである。そのためには、脳科学、音響学、心理学、医学、メディア芸術など多様な領域にわたる非分化全方位型の研究開発活性が必要となる。呈示システム、コンテンツ設計などにも未知の課題が多い。そうした課題をひとつひとつ検討しつつ、困難ながら大きな展望のあるこの課題に取組んでいきたいと考えている。

文献

1) 大橋　力、2003、至福の音体験と脳――全方位非分化型アプローチの射程から、小泉英明編著、脳科学と芸術、工作舎、270–290。
2) 大橋　力、2003、音と文明――音の環境学ことはじめ、岩波書店。
3) Oohashi T, Nishina E, Kawai N, et al., 1991, High frequency sound above the audible range affects brain electric activity and sound perception, AES 91st Convention, Preprint 3207.
4) 大橋 力、渡辺一成、服部和徳、1984、非定常音の高域制限による音質変化検知について、日本音響学会聴覚研究会資料、H-84-42、1-4。
5) Oohashi T, Nishina E, Honda M, Kawai N, Shibasaki H et al., 2000, Inaudible high-frequency sounds affect brain activity: Hypersonic effect, J of Neurophysiology 83, 3548-3558.
6) Friston K J, et al., 1995, Statistical parametric maps in functional imaging: a general linear approach, Human Brain Mapping 2, 189-210.
7) 大橋 力、河合徳枝、本田 学、仁科エミ、八木玲子他、2003、ハイパーソニック・エフェクトの生理学、AES 東京コンベンション 2003、94-97。
8) Yagi R, Nishina E. & Oohashi T, 2003, A method for behavioral evaluation of the"hypersonic effect", Acoustical Science and Technology 24,197-200.
9) Ohashi T, Kawai N, Nishina E, Honda M, Yagi R, Yonekura Y, Shibasaki H et al, 2006, The role of biological system other than auditory air-conduction in the emergence of the hypersonic effect, Brain Research 1073-1074, 339-347.
10) 仁科エミ、大橋力、2007、ハイパーソニック・エフェクトを応用した市街地音環境の改善とその生理・心理的効果の検討、日本都市計画学会都市計画論文集、42-3、139-144。
11) Hypersonic Blu-ray Disc "AKIRA" 、2010、バンダイビジュアル、BCXA-0001。

ハイパーソニック・エフェクト応用による音響療法の予備的検討

A preliminary research on "sound therapy" as an application of hypersonic effect.

○八木玲子[1),2)], 仁科エミ[3)], 河合徳枝[1)], 森本雅子[2)], 上野 修[2),4)], 本田 学[2),4)], 大橋 力[1)]

1) 国際科学振興財団, 2) 国立精神・神経医療研究センター,
3) 放送大学／総合研究大学院大学, 4) 科学技術振興機構 CREST

YAGI Reiko[1),2)], NISHINA Emi[3)], KAWAI Norie[1)], MORIMOTO Masako[2)], UENO Osamu[2)], HONDA Manabu[2),4)], OOHASHI Tsutomu[1)]

(Foundation for Advancement of International Science[1)], National Center of Neurology and Psychiatry[2)], The Open University of Japan/Sokendai[3)], CREST, JST[4)])

知覚限界をこえ、非定常なゆらぎ構造をもつ超高周波成分を含む音——ハイパーソニック・サウンドによる基幹脳活性化効果"ハイパーソニック・エフェクト"の臨床応用の可能性を探ることを目的として、精神科領域の一症例を対象に、臨床研究に向けた探索的・予備的検討を行った。生理指標、心理指標、行動指標を組み合わせた複合評価の結果から、本研究の対象者であるうつ病患者において、ハイパーソニック・サウンドの呈示が心身をリラックスさせ、不安を低減する効果をもつ可能性が示唆された。

Key Words: sound therapy, hypersonic effect, hypersonic sound, depression

1 はじめに

私たちは、人間の可聴周波数上限の 20kHz をこえ、非定常なゆらぎ構造をもつ超高周波成分を豊富に含む音——ハイパーソニック・サウンドによる基幹脳活性化効果"ハイパーソニック・エフェクト"[1),2)]を応用して心身の状態の改善をはかる<音響療法>について、精神科領域における臨床応用の可能性を探る予備的検討をはじめている。本研究では、気分障害の一症例を対象にした試みについて報告する。

2 方法

2.1 対象症例

39 歳男性。臨床診断はうつ。薬物療法を中心とした通院治療を継続しつつ、投薬効果が不十分なため、投薬以外の治療法の試みを希望し、X-1 年 12 月から X 年 7 月までの 8 ヶ月間、計 16 回の実験に参加した。実験開始の約 1 ヶ月前の X-1 年 10 月末に、転地療法により症状の改善が見られたため、主治医判断により抗うつ薬（セルトラリン）の服用を終了。実験期間中は、睡眠導入剤（ゾルピデム）および抗不安薬（ロフラゼプ酸エチル）の内服を継続。4 月中旬～下旬の約 2 週間、会社の組織変更による適応困難を生じた際、セルトラリンを頓服したほか、頓服用頭痛薬を処方されている。その他の投薬量に変化はない。

実験開始時の State-Trait Anxiety Inventory（以下、STAI）[3)]を用いた特性不安の測定値は、52 点（IV群「高い」とV群「非常に高い」との境界）、機能の全体的評定尺度(Global Assessment of Functioning Scale; GAF 尺度)[4)]は 70。実験開始時点では休職していたが、X 年 2 月より復職し、X 年 7 月に至る。

2.2 呈示刺激

実験には、健常者を対象とした先行研究で、ハイパーソニック・エフェクトを統計的有意に発生させるハイパーソニック・サウンドであることが検証された音源を用いた[5)]。

具体的には、可聴域上限をこえ非定常な超高周波

成分を豊富に含む熱帯雨林の自然環境音を、高速標本化 1 ビット量子化方式[6]でデジタル録音した 20 分間の音試料を呈示した。Fig. 1 に、実験に用いた音源の平均パワースペクトルを示す。

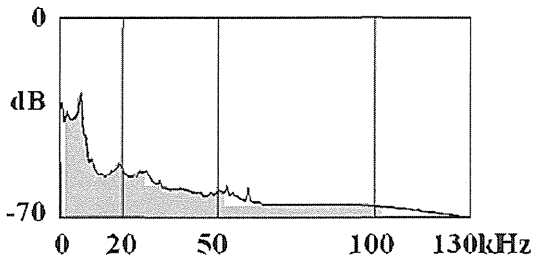

Fig. 1 実験に用いた音源のパワースペクトル

2.3 呈示装置

可聴域上限を大きく上回る超高周波成分を含む音源を高忠実度で再生するために、100kHz までほぼ平坦な再生特性をもつ音響呈示システムを構築した (Fig. 2)。

100kHz まで良好な特性をもつ高速標本化 1 ビット量子化方式のプレーヤから出力した音源の電気信号を、同じく 100kHz まで良好な周波数応答をもつアンプを経由し、約 3 m の距離をおいて配置した左右のスピーカから呈示した。実験室内の調度および温湿度は、被験者が快適な状況で実験に臨めるよう配慮した。

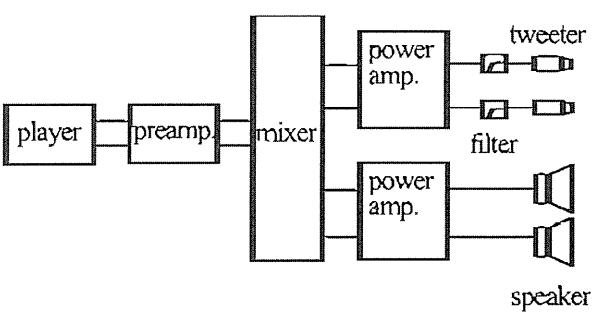

Fig.2 実験システムのブロックダイアグラム

2.4 実験プロトコル

対象者は、左右のスピーカから約 3 m の位置で安楽に座位をとり、呈示される自然環境音のハイパーソニック・サウンドを 20 分間受容した。

受容の前後に、生理指標として血圧・心拍数、心理指標として STAI を用いた状態不安検査、行動指標として精神テンポをそれぞれ測定した。精神テンポは、パーソナルテンポ (personal tempo) とも呼ばれ、特定の制約のない行動場面で自然に表出される個人固有の生体リズムの速度と考えられている。精神状態により変動することが知られており，変動要因が除去されると、時間の経過とともに元の速度に戻る恒常性を持つとの報告もある[7,8]。ただしその生理学的意義については不明な点も多いため、今回は簡便に計測可能な探索的指標として導入した。

全 16 回の試行前後に計測した各指標について、対応のある 2 群の t 検定を用いて統計検定を行った。

また、X 年 4 月から、対象者の病状の変化を把握するために、実験開始に先立って、うつ病 (抑うつ状態) 自己評価尺度 (Center for Epidemiologic Studies Depression Scale; 以下 CES-D)[9] を用いたうつ症状の評価を行った。

2.5 倫理的配慮

本研究は、国立精神・神経医療研究センター倫理委員会の承認を得て実施した。

本研究に参加しない主治医に実験の目的と内容をあらかじめ説明し、主治医により実験参加に可能な臨床状態と判断された症例を対象とした。

実験参加に先立ち、対象者に対して、研究目的、内容、および本研究に参加しないことや途中で中断することが本人に何ら不利益をもたらさないことを口頭および文書にて説明し、書面による同意を得て研究を実施した。

3 結果

3.1 生理指標

音響療法前後における血圧および心拍数の変化を Fig. 3～Fig. 5 に示す。

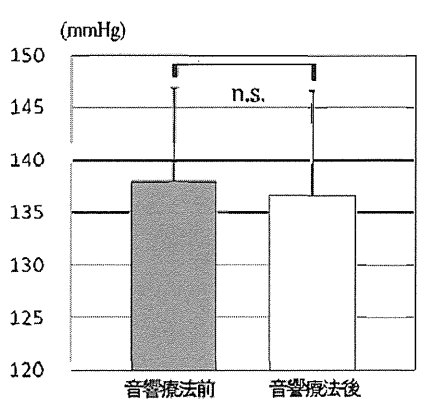

Fig.3 収縮期血圧の変化

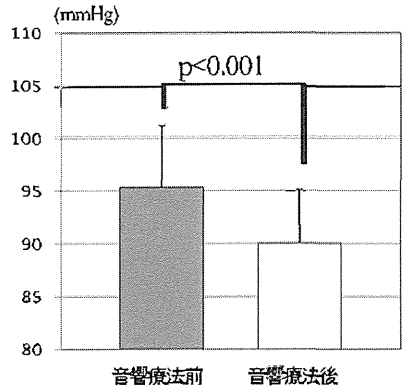

Fig.4 拡張期血圧の変化

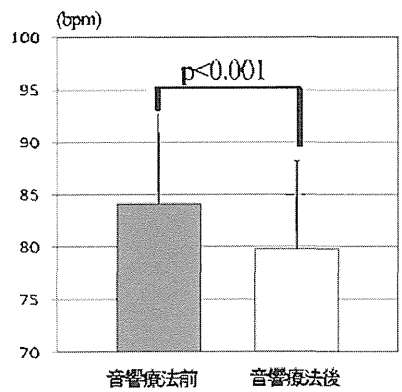

Fig.5 心拍数の変化

音響療法前後で、収縮期血圧（Fig. 3）は統計的有意な変化は認められなかったが、拡張期血圧（Fig. 4）および心拍数（Fig. 5）は、本研究対象者個人内において有意に低下した（拡張期血圧 $p<0.001$、心拍数 $p<0.01$）。

3.2 心理指標

3.2.1 状態不安

音響療法前後の状態不安の変化を Fig. 6 に示す。

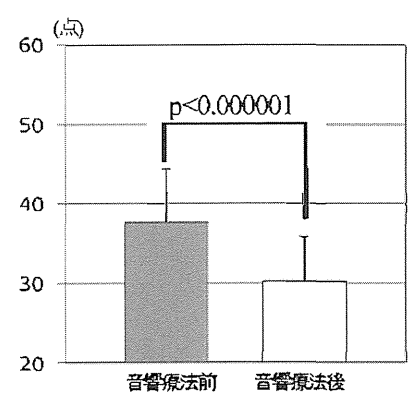

Fig. 6 状態不安の変化

全 16 試行の状態不安の平均値は、音響療法前が 37.69 点に対して音響療法後は 30.25 点を示し、音響療法前後で平均 7.44 点低減した。また統計的有意性は $p<0.000001$ というきわめて高い水準を示した。

3.2.2 うつ症状

対象者の病状の全体的な変化を把握する目的で、X 年 4 月～7 月の 4 ヶ月間、全 8 回にわたり、実験に先立って行った CES-D を用いたうつ症状評価の変化を Fig. 7 に示す。

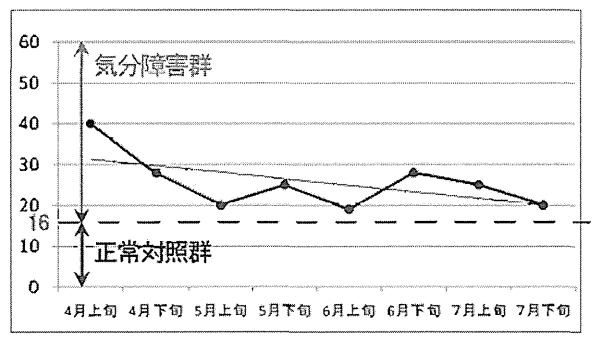

Fig.7 うつ症状評価の変化

うつ症状の自己評価値は、何度かの揺り戻しを経つつ、統計的有意性には達しないものの、全体としては軽減傾向にあることが認められる（$p=0.127$）。6 月下旬にうつ症状の評価値が上昇しているのは、会社での人間関係にストレスを感じているとの対象者の自己申告を反映しているものと看做される。

3.3 行動指標

音響療法前後の精神テンポの変化を Fig. 8 に示す。全 16 試行の精神テンポの平均値は、音響療法前が 55.06bpm、音響療法後が 54.69bpm であり、両者の間に統計的な有意差は認められなかった。

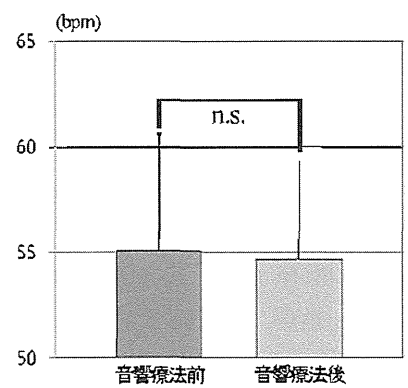

Fig. 8 精神テンポの変化

4　考察

以上の結果から、これまで、健常者を対象とした実験において、基幹脳血流の増大や免疫力の向上、快適性の向上、接近行動の誘導などを統計的有意に導くことが明らかになっているハイパーソニック・サウンドが、本研究の対象者であるうつ病患者においても、少なくとも負の影響を及ぼす可能性は低く、むしろ心身をリラックスさせ、不安を低減させる効果をもつ可能性をもつことが示唆された。

今回の検討は、対象者の心身の状態を改善することを主眼に、ごく探索的な試みを行ったにすぎず、実験条件の設定、対照条件の設定、方法の整備等は今後の課題である。こうした探索的段階であるにもかかわらず、ハイパーソニック・エフェクトの臨床的効果を否定できない結果が得られたことには、注目してよいのではないかと考える。

今後は、まず、適切な実験条件、指標の探索など基本的な実験方法の整備に取り組み、症例を増やして、ハイパーソニック・エフェクトの臨床応用に向けた有効性を確かめていきたいと考えている。

参考文献

1) Oohashi T. et al. (2000) Inaudible high-frequency sounds affect brain activity, A hypersonic effect, Journal of Neurophysiology, 83, 3548-3558.
2) Oohashi T. et al. (1991) AES High Frequency Sound Above the Audible Range Affects Brain Electric Activity and Sound Perception, Audio Engineering Society 91st Convention (New York) Preprint 3207, 1-25.
3) 水口 公信 他 (1991) 日本版 STAI 状態・特性不安検査 使用手引, 三京房.
4) 高橋 三郎 他訳(2003) DSM - IV - TR 精神疾患の診断・統計マニュアル, 医学書院
5) 仁科 エミ 他 (2005) 超高密度高複雑性森林環境音の補完による都市音環境改善効果に関する研究—脳波, 血中性活性物質, 主観的印象評価の組み合わせによる評価, 日本都市計画学会都市計画論文集, No.40-3, 169-174.
6) 山崎 芳男 他 (1994) 広帯域音響信号の高速標本化 1bit 処理, 電子情報通信学会 信学技報, EA93-102.
7) Gotor, P. (1934) The Personal Tempo in Psychopathology (El tempo personal en psicopatologia), Arch. de Neurobiol., vol. xiv, 363.
8) 杉之原 正純 他 (1982) 精神テンポに関する基礎的研究(7), 広島修大論集, 第23 巻, 第2 号, 120.
9) L. S. Radloff (2000) Center for Epidemiologic Studies Depression Scale (CES-D). Modified From: Rush J, et al: Psychiatric Measures, APA.

謝辞

本研究にあたり、実験参加者の紹介および情報提供の労をおとりくださった精神科医の小栗 淳先生、実験の実施にあたり、対象者のケアにあたってくださった精神保健福祉士の植村麻紀氏、そして、実験に快くご協力くださった患者さまに、厚く御礼申し上げます。

ASIAGRAPH 2010

ハイパーソニックブルーレイディスク『AKIRA』

Hypersonic sound track for Blu-ray Disc "*AKIRA*"

仁科エミ/放送大学,総合研究大学院大学, 森本雅子/国立精神・神経医療研究センター, 福島亜理子/東京大学, 八木玲子/国際科学振興財団

NISHINA Emi[1]/ Open University of Japan, The Graduate University for Advanced Studies, MORIMOTO Masako[2]/ National Center of Neurology and Psychiatry, FUKUSHIMA Ariko[3]/The University of Tokyo, YAGI Reiko[4]/ Foundation for Advancement of International Science

*[1]nishina@ouj.ac.jp, *[2]morimoto@ncnp.go.jp, *[3]ariko@cyber.t.u-tokyo.ac.jp, *[4]yagi@fais.or.jp

Abstract: The hypersonic Blu-ray Disc "*AKIRA*", an animation film directed by OTOMO Katsuhiro, created to deliver superior content, born of an unprecedented level of information density, offering lush visuals and mind-blowing sound that transports the audience to a place of pleasure and awe that is moving and intoxicating at the same time. The authors reported the making process of its sound track for Blu-ray Disc to discuss the new requirement of the sound reproduction system in home theater.

Keywords: Hypersonic Effect, Animation movie, Sound track, High frequency components

1. Introduction

The animation film "*AKIRA*", directed by Japanese famous *manga* creator OTOMO Katsuhiro, swept across the world, flooring audiences everywhere in the blink of an eye after its 1988 theatrical release, and this historic film retains a massive fan base to this day. Some 20 years after its release, we see that the near future it depicted—one of concerted terrorist attacks, the destruction of Earth's environment, natural disasters, widespread strife, and an array of ailments of the soul, eroding at the hearts of mankind—has steadily become reality. The film's apocalyptic vision has proven acutely prophetic.

This animated film was published as Laser Disc and VHS video in 1988 with stereo sound track. For its transition to DVD in 2001, 5.1ch sound track has re-mastered by YAMASHIRO Shoji, the composer of the music in this film. In 2009, *AKIRA* on Blu-ray disc offers

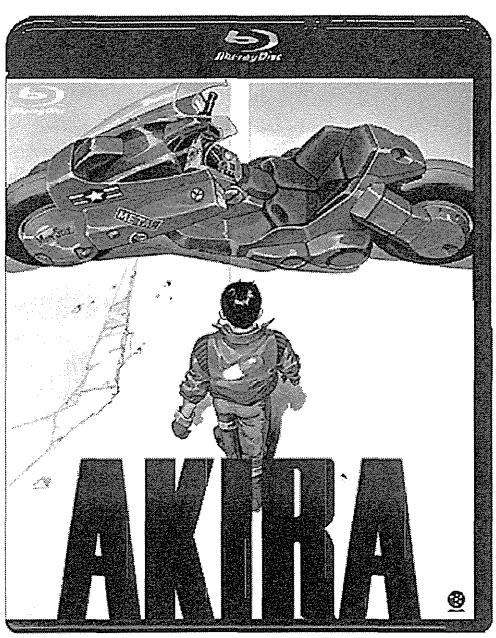

Figure 1: Bly-ray Disc "*AKIRA*" directed by OTOMO Katsuhiro

the film's original Japanese audio in 5.1ch sound, maximizing the potential of the media's 192 kHz sampling / 24 bit coding audio specs to capture hypersonic sound, a source of sound that includes ultra-high frequencies exceeding 90kHz.

In this paper, as the member of this project, we would like to report the making process of the sound track of Bly-ray Disc *AKIRA* to discuss the new requirement of the sound reproduction system in home theater.

2. What is the "Hypersonic effect" ?

For the film's transition to Blu-ray Disc ("BD"), 192 kHz-sampled / 24 bit-quantized audio was selected with the finding of "Hypersonic Effect" by OOHASHI Tsutomu, that is the real name of Composer YAMASHIRO.

As is widely known, the upper limit of audible frequency for aerial vibration is approximately 15 kHz (15,000 cycle per second) for ordinary people. There are only a few people who can recognize a frequency of 20 kHz or higher. However, there are myriad sounds on Earth that generate intricately changing, high-frequency components above the so-called audible range. Gamelan music of Bali Island and environmental sounds in tropical rain forests are examples of such sounds; these data are extremely rich in high frequency components of more than 100 kHz. By carefully observing listeners being showered with

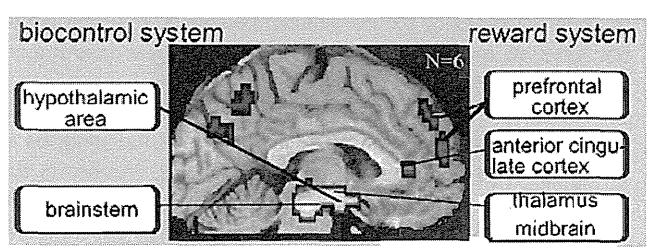

Figure 2: The fundamental brain network significantly activated by the sounds containing high frequency components above the human audible range